Journal of Alloys and Compounds 509 (2011) 4414–4419

Contents lists available at ScienceDirect

Journal of Alloys and Compounds

journal homepage: www.elsevier.com/locate/jallcom

Analysis of current–voltage characteristics of Al/p-$ZnGa_2Se_4$/n-Si nanocrystalline heterojunction diode

I.S. Yahia [a,b,*], M. Fadel [a], G.B. Sakr [a], F. Yakuphanoglu [b,c], S.S. Shenouda [a], W.A. Farooq [c]

[a] Department of Physics, Faculty of Education, Ain Shams University, Roxy, Cairo, Egypt
[b] Department of Metallurgical and Materials Engineering, Firat University, Elaziğ, Turkey
[c] Department of Physics and Astronomy, College of Science, King Saud University, Riyadh, Saudi Arabia

ARTICLE INFO

Article history:
Received 22 October 2010
Received in revised form 4 January 2011
Accepted 7 January 2011
Available online 15 January 2011

Keywords:
$ZnGa_2Se_4$ defect chalcopyrite
Thin film
XRD and AFM
Nanostructure heterojunction diode
Current–voltage characteristics

ABSTRACT

The polycrystalline $ZnGa_2Se_4$ thin film was prepared by thermal evaporation technique on n-Si wafer followed by annealing at 700 K. Then, the Al/p- $ZnGa_2Se_4$/n-Si/Al heterojunction diode was fabricated. XRD pattern shows that the annealed $ZnGa_2Se_4$ film has a polycrystalline structure. AFM images indicate that the $ZnGa_2Se_4$ film is formed of nanoparticles. The dark current–voltage characteristics of the heterojunction diode at various temperatures have been investigated to determine the electrical parameters and conduction mechanism. The Al/p-$ZnGa_2Se_4$/n-Si/Al diode shows a rectification ratio of 2.644×10^2 at ± 2 V at room temperature. It was found that at forward bias voltages ≤ 0.5 V, the conduction mechanism of the diode is controlled by the thermionic emission mechanism, while at bias voltages higher than 0.5 V, it is controlled by the space charge limited current mechanism. The series resistance R_s, the ideality factor n and the barrier height ϕ_b values of the diode are determined by performing different plots from the forward current–voltage characteristics. The reverse current mechanism of the diode is controlled by the carrier generation–recombination process in the depletion region. The obtained results show that the Al/p-$ZnGa_2Se_4$/n-Si/Al heterojunction is a good candidate for the electronic device applications.

1. Introduction

The chalcopyrite compounds are characterized by a chemical formula II–IV–V_2 and I–III–VI_2 and these compounds can be derived from a parent compounds III–V and II–VI, respectively, by replacing the group-III element by alternating a group-II and group-IV element or the group II by a group-I and group-III element. The most common examples of these compounds are $ZnGeP_2$ and $AgGaSe_2$, respectively, and these compounds exhibit a tetrahedral bonding derived from the zinc-blend crystal structure. The local valence is maintained as long as each group-V anion is surrounded by two group-II and two group-IV cations. The chalcopyrite structure corresponds to a particular ordering of the two types of cation [1]. Another class of tetrahedrally bonded materials is known as the defect chalcopyrites, which can be considered "ordered vacancy" compounds. For example, in a I–III–VI_2 compound, we may have the double formula unit and then remove one of the group-I elements, thus creating a vacancy and replacing the other group-I back by a group-II element to maintain the valence [2,3].

Defect chalcopyrite ordered vacancy compounds are a class of high technological materials due to their interesting semiconducting properties, broad band gaps, and potential applications in linear, nonlinear optical and photovoltaic devices [4]. $ZnGa_2Se_4$ is one of these semiconductors, which is a photosensitive material [5] and it can be used for phase change memories (PCMs) [6].

Our previous work on the amorphous $ZnGa_2Se_4$ defect chalcopyrite thin films suggests that $ZnGa_2Se_4$ is a good candidate for memory switching (phase changes from amorphous to crystalline) devices [6]. It is found that the dc electrical activation energy and the mean value of the threshold activation energy are 0.72 eV and 0.257 eV, respectively. The obtained values for the switching characteristics of the studied thin films were interpreted by electrothermal model [6]. Also, the ac electrical conductivity and the dielectric properties of $ZnGa_2Se_4$ thin films were studied. It is found that the ac conductivity is obeyed to power law $\sigma_{ac}(\omega) = B\omega^S$, in accordance with the hopping model and the frequency exponent s is found to be a temperature dependent and its value decreases slightly with increasing temperature. Accordingly, the ac conductivity can be interpreted in terms of the correlated barrier hopping (CBH) model. The dielectric constant and dielectric loss were found to decrease with increasing frequency. Our results support the correlation between ac conductivity and dielectric properties as suggested by Giuntini et al. [7,8].

---

[*] Corresponding author at: Department of Physics, Faculty of Education, Ain Shams University, Roxy, Cairo, Egypt. Tel.: +20 182848753; fax: +20 22581243.
E-mail addresses: dr_isyahia@yahoo.com, dr_isyahia@hotmail.com, isyahia@gmail.com (I.S. Yahia).

0925-8388/$ – see front matter © 2011 Elsevier B.V. All rights reserved.
doi:10.1016/j.jallcom.2011.01.068

The difference between the studied diode and other materials comes from the $ZnGa_2Se_4$, which is a new promising material; because we succeeded in the preparation of this material with high quality in both powder and thin film forms. Our previous work on $ZnGa_2Se_4$ can be used for phase change materials and also it can be used as solar windows instead of CdS to remove Cd from the solar cell devices due to its toxicity due to its wide bandgap (2.54 eV).

Thus, in present work, it is believed to be useful for the fabrication of $ZnGa_2Se_4$ thin films to show the application of this semiconductor material in electronic technology as a diode. With this aim, the Al/p-$ZnGa_2Se_4$/n-Si/Al heterojunction diode was fabricated for the first time. The dark current–voltage characteristics of the heterojunction diode at various temperatures have been investigated to determine the electronic conduction mechanism and to extract the electrical parameters of this diode.

2. Experimental details

The $ZnGa_2Se_4$ was prepared by the melt and slowly cooled technique using different thermal treatments. The constituent elements Zn, Ga and Se of high purity (99.999%), were weighed according to their stoichiometric ratio and sealed into an evacuated silica tube in a vacuum better than 2×10^{-5} Torr and then heated in home-made designed oscillatory furnace. The temperature of the furnace was increased by steps to 303, 490, 693 and 1423 K with a rate of 100 °C/h and was kept constant at each step for 2 h. Then, the sample was gradually cooled down, until it reached the following temperatures 873, 773 and 643 K and was kept constant for 1 h at each stage [9]. Finally, the sample was slowly cooled by the same rate of rising to reach to room temperature. The long duration of synthesis and mechanical shaking of the mixture in the oscillatory furnace provide the high homogeneity of the investigated compound. n-Type Si wafer was cleaned through the standard methodology to remove the native oxide [10].

Thin film of $ZnGa_2Se_4$ was grown by thermal evaporation technique (Edward's E 306A) onto the highly polished and cleaned glass and n-Si single-crystal substrates. The substrates were placed on a flat holder rotated horizontally for the more homogeneity of the film. The vacuum chamber was pumped down to 2×10^{-5} Torr. The temperature of the compound was then raised until the whole material evaporated with a deposition rate of about 2.5 nm/s. Film thickness was controlled using a thickness monitor (Edward FTM5), and then measured accurately by employing Tolansky's method of multiple-beam Fizeau fringes [11] and it was found to be 179 nm. The samples were annealed at 700 K for 1 h to obtain a polycrystalline structure. Then, Al electrodes were deposited by the thermal evaporation technique using a suitable point contact mask of radius 3 mm. The thickness of Al for the upper and lower electrodes is about 100 nm.

For X-ray diffraction (XRD) analysis of the annealed films on glass, investigated samples, Philips X-ray diffractometer (model X'-Pert) was used for the measurement by utilizing monochromatic CuK_α radiation operated at 40 kV and 25 mA. The elemental composition of the as-deposited thin film was determined using scanning electron microscope (Joel-JSM 5400) with EDX unit (Oxford), operating at an accelerating voltage of 30 kV. The elemental analysis of the as-deposited thin film leads to the chemical formula $Zn_{1.011}Ga_{1.994}Se_{3.995}$ revealing the nearly stoichiometric compound. AFM micrographs were investigated by Park System XE-100E atomic force microscopy (AFM) for $ZnGa_2Se_4$/n-Si. The analysis of the grain size was done by Park system XEI software.

The current–voltage (*I–V*) measurements were performed using a computer controlled Keithley 4200-SCS semiconductor characterization system. Two terminal cables of this device with SMU1 and SMU2 were connected to the specially designed holder for a point contact made from brass. The diameter of the upper and bottom electrodes is about 0.2 and 15 mm, respectively. The sample temperature was controlled using a Lakeshore 331 auto-tuning temperature controller with sensitivity better than ±0.1 K.

3. Results and discussion

3.1. Structure characterization

X-ray diffraction pattern of the $ZnGa_2Se_4$ thin film annealed at 700 K is shown in Fig. 1(a). XRD pattern indicates that the $ZnGa_2Se_4$ thin film has a polycrystalline with tetragonal structure. The preferred orientation plane for the film was determined to be (1 1 2).

Also, the observed minor peaks of other reflecting planes are (2 0 4) and (3 1 2). The unit cell lattice parameters were determined from the obtained data for the reflecting planes (1 1 2), (2 0 4) and (3 1 2). The lattice parameter *a* and *c* were found to be 5.704 and 10.481 Å, respectively. These values are in good agreement with those for the powder and the reported values [12]. The crystallite size *L* can be calculated from the full width at half maximum (FWHM) of the (1 1 2) peak using Debye–Scherrer formula [13]:

$$L = \frac{0.9\lambda}{\beta \cos\theta} \tag{1}$$

where β is the FWHM, λ is the wavelength of CuK_α radiation and θ is the angle. The calculated crystallite size *L* was found to be 61 nm. This suggests that the $ZnGa_2Se_4$ film is a nanostructure material.

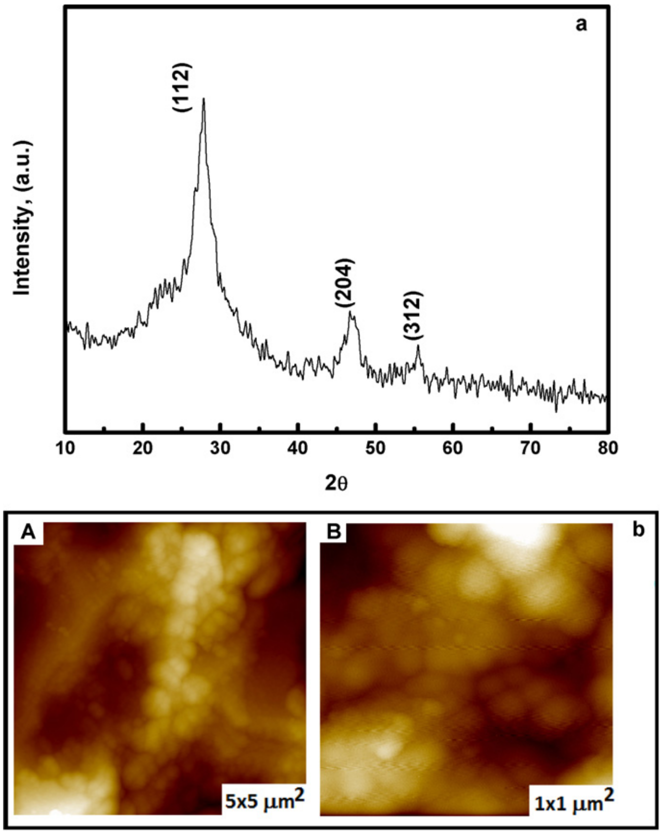

Fig. 1. (a) XRD pattern of $ZnGa_2Se_4$ film annealed at 700 K. (b) AFM micrographs in 2D (A) 5 × 5 and (B) 1 × 1 μm².

The structural properties of the $ZnGa_2Se_4$ film were investigated by AFM images. AFM images of 5 × 5 and 1 × 1 μm² in two dimensional scales (2D) are shown in Fig. 1(b). As seen in Fig. 1(b), the film is formed of nanoparticles having cluster form. This confirms that the $ZnGa_2Se_4$ film is nanostructure material. The type of nanostructure particles is like spherical shape. The grain size for the $ZnGa_2Se_4$ film was found to be 68.02 nm using Park system XEI software programming.

3.2. Current–voltage characteristics

The electrical conductivity type of the $ZnGa_2Se_4$ was determined by hot probe method. The hot probe result indicates that the $ZnGa_2Se_4$ exhibits p-type electrical conductivity. After this characterization, Al/p-$ZnGa_2Se_4$/n-Si/Al heterojunction was fabricated and *I–V* characteristics of the heterojunction diode at various temperatures are measured, as shown in Fig. 2. From this figure, it is observed that the diode exhibits a rectifying behavior with a rectification ratio (*RR*) which is ratio of the forward current to the reverse current at a certain applied voltage. The *RR* value for the diode was found to be 2.644×10^2 at ±2 V and also, the diode has a high forward resistance ~20 kΩ at 2 V. This high resistance value affects the current–voltage behavior of the diode. Thus, we have to deter-

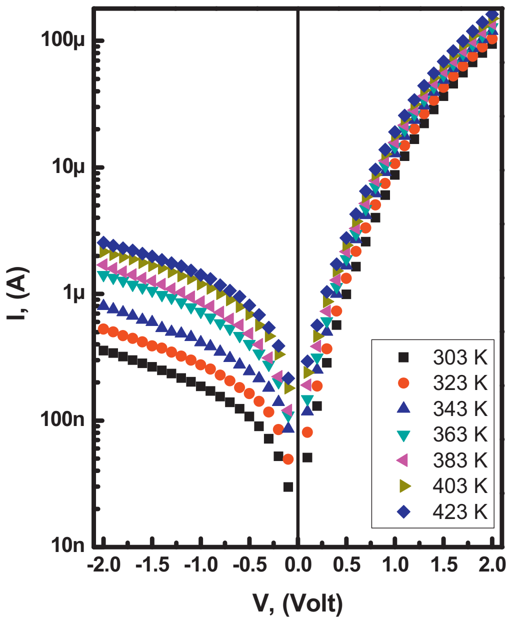

Fig. 2. *I*–*V* characteristics of p-ZnGa$_2$Se$_4$/n-Si heterojunction at different temperatures.

mine the parasitic resistances such as series resistance and shunt resistance. For this, we can use the following relation:

$$R_j = \frac{\partial V}{\partial I} \tag{2}$$

where R_j is the junction resistance. The values of series R_s and shunt R_{sh} resistances are determined by plotting the junction resistance R_j as a function of forward and reverse biasing voltages for each temperature. At the higher forward voltages, the junction resistance arrives to a constant value, which equals to R_s. The same behavior occurs also in reverse biasing voltages leading to determine the value of R_{sh}. The determined values R_s and R_{sh} are given in Table 1. The values of the series resistance R_s (resistance of the diode material and metallic contacts) and the shunt resistance R_{sh} (responsible for the lost current at the edge of the device and the surface inhomogeneities) at room temperature are 21 kΩ and 5.6 MΩ, respectively. The R_s and R_{sh} values have a crucial importance effect on the performance of the diode. The magnitude of both resistances decreases with increasing temperature. This effect is probably associated with the increase of the free carriers density available in the junction, due to either the bond breaking effect or the detrapping mechanism [14,15].

It is evaluated that at the forward bias voltages, the diode exhibits two conduction mechanisms operating in various bias voltage ranges. The first mechanism takes place in voltages, $V \le 0.5$ V. For analysis of this mechanism, the relation between $\ln I_f$ and low forward bias voltage ($V \le 0.5$ V) at different temperatures is shown in Fig. 3. As seen in Fig. 3, at lower voltages, the forward current of the diode increases exponentially with increasing biasing voltage. Thus, it can be evaluated that the Al/p-ZnGa$_2$Se$_4$/n-Si/Al heterojunction behaves like a Schottky diode [16].

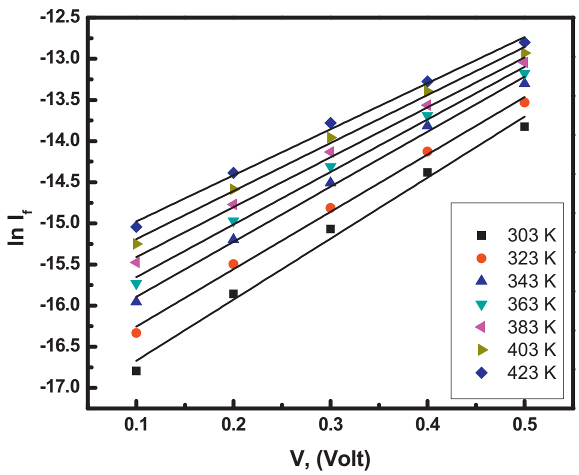

Fig. 3. Variation of $\ln I_f$ versus V for Al/p-ZnGa$_2$Se$_4$/n-Si/Al heterojunction diode at potentials ≤0.5 V.

In that case, the current–voltage characteristics of the diode can be analyzed by the following relation [14]:

$$I = I_s \exp\left(\frac{eV}{nk_BT}\right) \tag{3}$$

where n is the ideality factor diode, e is the electronic charge, k_B is the Boltzmann constant and I_s is the reverse saturation current given by the following relation [17,18]:

$$I_s = AA^*T^2 \exp\left(-\frac{e\phi_b}{k_BT}\right) \tag{4}$$

where A is the diode contact area, A^* is the Richardson constant ($A^* = 112$ A/cm^2 K^2 for n-Si [19,20]) and ϕ_b is the barrier height. The n values of the diode were determined from the slope of Fig. 3 at various temperatures using the relation $n = (e/k_BT)(dV/d(\ln I_f))$ and are shown in Fig. 4. It is observed that n value is decreased with increasing temperature. The obtained n value is higher than unity indicating that there is a deviation from the ideality behavior. The deviation of n from unity may be attributed to either recombination of electrons and holes in the depletion region, and/or increase of diffusion current due to increase of applied voltage [21]. The values of ϕ_b were calculated by means of $\phi_b = (k_BT/e)\ln(AA^*T^2/I_s)$. The variation of ϕ_b with temperature is shown in Fig. 4. It is seen that the value of ϕ_b increases with increasing temperature. As the temperature increases, more and more carriers have sufficient energy to surmount the higher barriers [22]. As a result, the dominant barrier height is increased with the temperature [23]. This type of dependency of the ideality factor and the barrier height on temperature can be explained by the inhomogeneous of barrier height and/or the interfacial layer of the metal–semiconductor [24].

Table 1
Electrical parameter of Al/p-ZnGa$_2$Se$_4$/n-Si/Al heterojunction diode.

T (K)	R_j–V		I–V					$F(V)$–V	
	R_s (kΩ)	R_{sh} (MΩ)	n	ϕ_b (eV)	m	l	T_t (K)	ϕ_b (eV)	R_s (kΩ)
303	21.197	5.605	5.161	0.843	3.432	2.432	736.835	0.871	38.623
323	19.229	3.787	5.149	0.890	3.290	2.292	739.670	0.916	32.364
343	16.751	2.503	5.055	0.937	3.207	2.207	756.864	0.959	27.890
363	15.532	1.412	5.001	0.986	3.166	2.166	786.331	1.007	27.559
383	14.669	1.181	4.993	1.035	3.118	2.118	811.194	1.054	25.820
403	13.298	0.993	4.933	1.084	3.096	2.096	844.769	1.101	24.385
423	12.346	0.786	4.895	1.133	3.068	2.068	874.595	1.164	14.565

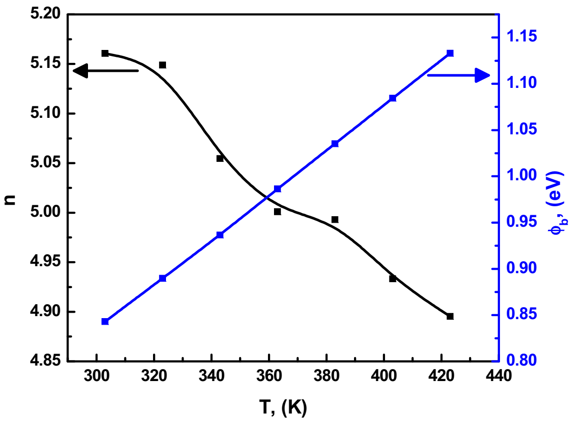

Fig. 4. Variation of the ideality factor and the barrier height as a function of temperature for Al/p-$ZnGa_2Se_4$/n-Si/Al heterojunction diode.

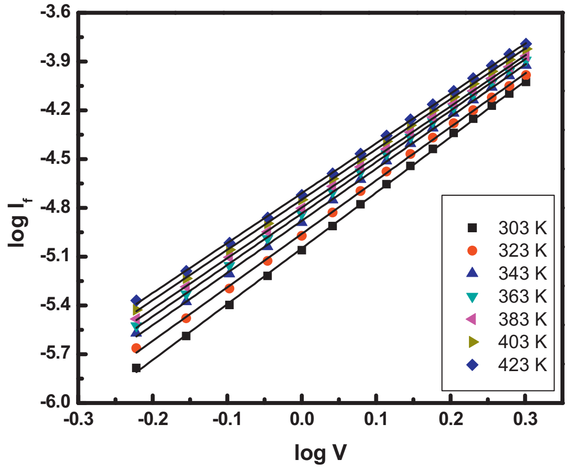

Fig. 5. Variation of log I_f versus log V at forward bias >0.5 V for Al/p-$ZnGa_2Se_4$/n-Si/Al heterojunction diode.

In order to determine the operating conduction mechanism, at higher bias voltages, $V \geq 0.5$ V, we plotted the curve of log I_f versus log V for various temperatures (see Fig. 5). The current mechanism was analyzed by power law, $I \alpha V^m$, here m is an exponent determining the conduction mechanism. The exponent m values for the second region were calculated from the slopes of Fig. 5. The extracted values of m are decreased with increasing temperature, as shown in Table 1. This suggests that the conduction mechanism is controlled by a space-charge-limited current mechanism (SCLC). Therefore, the conduction mechanism can be expressed by the following relation [25,26]

$$I = \frac{eA\mu N}{d^{2l+1}}\left(\frac{\varepsilon\varepsilon_o}{eP_o k_B T_t}\right)^l V^{l+1} \qquad (5)$$

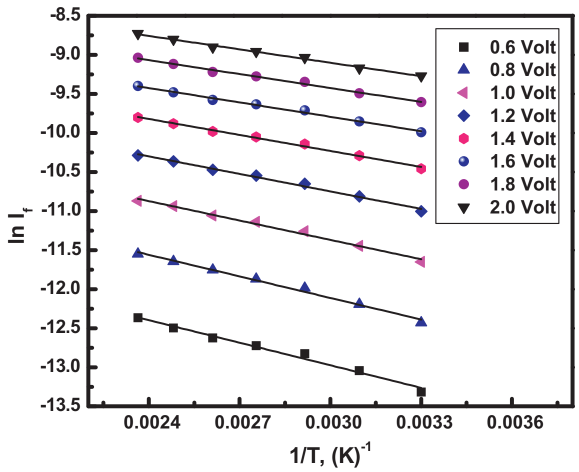

Fig. 6. Dependence of ln I_f on the reciprocal temperature $1/T$ at different biasing voltages for Al/p-$ZnGa_2Se_4$/n-Si/Al heterojunction diode.

where ε is the dielectric constant of the semiconductor, ε_o is the permittivity of free space, μ is the mobility of charge carriers, N is the effective density of states in the electronic band edge, d is the thickness of the sample, l is a parameter given by $l = m - 1 = T_t/T$, T_t is a characteristic temperature of the exponential distribution of the traps [27] and P_o is the trap density per unit energy range at the valence band. The values of l and T_t were calculated and are given in Table 1. The l value is decreased and T_t value is increased with increasing temperature. For the diode, the total concentration of trap states is obtained by the following relation [14]:

$$N_t = P_o k_B T_t \qquad (6)$$

In order to determine both N_t and P_o, the variation of ln I_f versus $1/T$ at various bias voltages was shown in Fig. 6. The slope of this plot can be analyzed according to the equation [14]:

$$\text{slope} = \frac{\Delta \ln I}{\Delta(1/T)} = T_t \ln\left(\frac{\varepsilon V}{ed^2 N_t}\right) \qquad (7)$$

With help of Eqs. (6) and (7), the values of N_t and P_o were calculated and given in Table 2. The N_t values increase with the applied voltage and temperature. Also, P_o increases with increasing the applied voltage due to thermally generated more charges. The obtained N_t values for the studied diode are higher than that of $ZnIn_2Se_4$/p-Si/Al heterojunction diode ($N_t = 3.12 \times 10^{25}$ m^{-3}) [28]. The difference between the trap concentrations of $ZnGa_2Se_4$ and $ZnIn_2Se_4$ is due to the presence of various trap levels in the forbidden band gaps of the $ZnGa_2Se_4$ and $ZnIn_2Se_4$ materials.

Also, we used Norde method to determine the values of barrier height and series resistance [17,29–31]:

$$F(V) = \frac{V}{\gamma} - \frac{k_B T}{e}\ln\frac{I(V)}{AA^* T^2} \qquad (8)$$

Table 2
Values of N_t and P_o of Al/p-$ZnGa_2Se_4$/n-Si/Al heterojunction diode.

V (V)	N_t (10^{33} m^{-3})							P_o (10^{52} J m^{-3})
	At 303 K	At 323 K	At 343 K	At 363 K	At 383 K	At 403 K	At 423 K	
0.6	0.192	0.193	0.199	0.208	0.216	0.227	0.236	1.889
0.8	0.271	0.272	0.280	0.293	0.304	0.318	0.329	2.663
1.0	0.385	0.386	0.396	0.413	0.427	0.444	0.459	3.785
1.2	0.514	0.516	0.528	0.548	0.564	0.585	0.603	5.055
1.4	0.655	0.657	0.671	0.694	0.713	0.737	0.758	6.440
1.6	0.822	0.825	0.841	0.866	0.887	0.915	0.938	8.086
1.8	0.949	0.952	0.970	0.999	1.022	1.052	1.078	9.333
2.0	1.086	1.089	1.109	1.140	1.166	1.199	1.228	10.68

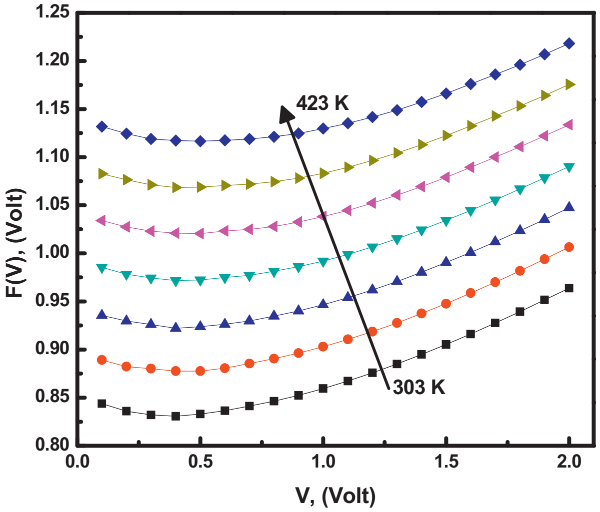

Fig. 7. Variation of $F(V)$ versus V at different temperatures for Al/p-$ZnGa_2Se_4$/n-Si/Al heterojunction diode.

where γ is the first integer (dimensionless) greater than n. According to our results, the value of γ is 6. For determination of R_s and ϕ_b values, the plots of $F(V)$ versus V at different temperatures are shown in Fig. 7. This figure gives a minimum point $F(V_o)$. The relation between the minimum point and the barrier height is expressed as [17,30,31]:

$$\phi_b = F(V_o) + \frac{V_o}{\gamma} - \frac{k_B T}{e} \tag{9}$$

where V_o is the corresponding voltage. Then, the values of R_s are determined by the following relation [17,30,31]:

$$R_s = \frac{k_B T(\gamma - n)}{eI_o} \tag{10}$$

The values of ϕ_b and R_s were determined and are given in Table 1. As seen in Table 1, the values of ϕ_b obtained from Eq. (9) are in good agreement with that obtained from the forward bias $\ln I_f$–V. Also, the values of R_s obtained from Eq. (10) and from the R_j–V method are approximately in the same order.

Also, the reverse current mechanism of the diode was analyzed. It is observed that the reverse current I_r has a small dependence on voltage, although it increases rapidly with temperature, indicating that I_r should be limited by another transport mechanism. It is evaluated that the reverse current due to carrier recombination is thermally activated and can be used by the following relation [32]:

$$I_r = I_{oo} \exp\left(\frac{-\Delta E}{k_B T}\right) \tag{11}$$

where ΔE is the carrier activation energy for conduction mechanism and I_{oo} is a constant. The plot of $\ln I_r$ versus $1000/T$ for the diode is shown in Fig. 8. The value of ΔE is determined from the slope of the straight lines, which has a mean value of 0.186 ± 0.009 eV. This indicates that the dominant mechanism for reverse current over the studied range of temperatures and voltages is the generation and recombination of carriers in the depletion region.

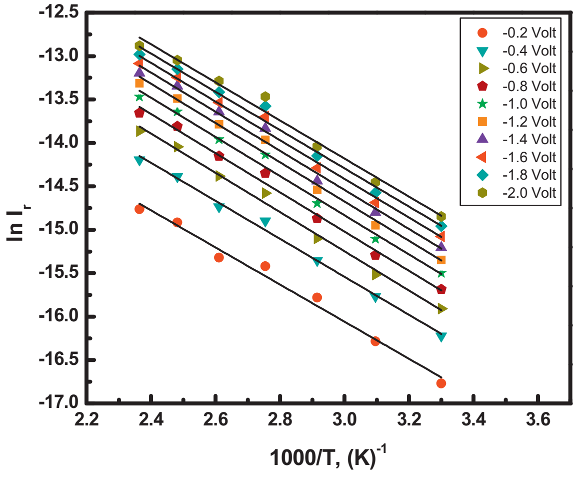

Fig. 8. Plot of $\ln I_r$ versus $1000/T$ for Al/p-$ZnGa_2Se_4$/n-Si/Al heterojunction diode in negative biasing voltages.

4. Conclusions

Hot probe test shows that the $ZnGa_2Se_4$ film is a p-type semiconductor. The nanostructure of the $ZnGa_2Se_4$ film was confirmed by means of XRD and AFM measurements. The dark current–voltage characteristics of the Al/p-$ZnGa_2Se_4$/n-Si/Al heterojunction show a rectification behavior. The current–voltage measurements suggest that the charge transport mechanism of the $ZnGa_2Se_4$/n-Si is controlled by two conduction mechanisms, thermionic emission (TE) at the lower forward voltages ($V \leq 0.5$ V) and space charge limited conduction (SCLC) at the higher forward voltages ($V > 0.5$ V). The diode exhibits a non-ideal behavior with ideality factor greater than unity. The reverse current is limited by the carrier generation–recombination process and thermally activated with an activation energy ΔE (0.186 ± 0.009 eV). Our work supports the electronic applications of $ZnGa_2Se_4$ in semiconductor devices.

Acknowledgements

This work was partially supported by the Management Unit of Scientific Research projects of Firat University (FÜBAP) (Project Number: 1947) and King Saud University under grant: KSU-VPP-102. One of the authors wishes to thank FÜBAP and KSU.

References

[1] X. Jiang, W.R.L. Lambrecht, Phys. Rev. B 69 (2004) 035201.
[2] J.X. Shu, M. Shu, S.P. Jun, L. Yuan, L.J. Qing, Chin. Phys. Lett. 26 (2009) 077102.
[3] S. Susanne, R. Uwe (Eds.), Wide-Gap Chalcopyrites, Series: Springer Series in Materials Science, vol. 86, 2006, p. XIV.
[4] T. Ouahrani, H. Ali, R. Reshak, B. Khenata, M. Amrani, A. Mebrouki, V. Otero-de-la-Roza, J. Luaña, Solid State Chem. 183 (2010) 46.
[5] A.M. Salem, W.Z. Soliman, Kh.A. Mady, Phys. B 403 (2008) 145.
[6] I.S. Yahia, M. Fadel, G.B. Sakr, S.S. Shenouda, J. Alloys Compd. 507 (2010) 551.
[7] M. Fadel, I.S. Yahia, G.B. Sakr, S.S. Shenouda, The 2nd International Conference on Advanced Materials and their Applications and its workshop on "New Trends on Nanoscience and Laser Physics", April 6–8, NRC, Cairo, Egypt, 2010.
[8] J.C. Giuntini, J.V. Zanchetta, D. Jullien, R. Eholie, P. Houenou, J. Non Cryst. Solids 45 (1981) 57.
[9] M. Morocoima, M. Quintero, E. Guerrero, R. Tovar, P. Conflant, J. Phys. Chem. Solids 58 (1997) 503.
[10] M. Soylu, F. Yakuphanoglu, J. Alloys Compd. 506 (2010) 418.
[11] S. Tolansky, Introduction to Interferometry, Longman, London, 1955.
[12] JCPDS-International Centre for Diffraction Data, Card Number (89-5716), 1998.
[13] B.D. Cullity, Elements of X-ray Diffraction, Addison-Wesley, Reading, MA, 1979.
[14] I.S. Yahia, G.B. Sakr, T. Wojtowicz, G. Karczewski, Semicond. Sci. Technol. 25 (2010) 095001.
[15] H. Uslu, A. Bengi, S.Ş. Çetin, U. Aydemir, Ş. Altındal, S.T. Aghaliyeva, S. Özçelik, J. Alloys Compd. 507 (2010) 190.
[16] Y. Caglar, M. Caglar, S. Ilıcan, F. Yakuphanoglu, Microelectron. Eng. 86 (2009) 2072.
[17] F. Yakuphanoglu, J. Alloys Compd. 494 (2010) 451.
[18] H. Uslu, S. Altındal, U. Aydemir, I. Dokme, I.M. Afandiyeva, J. Alloys Compd. 503 (2010) 96.
[19] Ş. Aydoğan, Ü. İncekara, A. Türüt, Thin Solid Films 518 (2010) 7156.
[20] A. Bengi, U. Aydemir, S. Altındal, Y. Ozen, S. Ozcelik, J. Alloys Compd. 505 (2010) 628.
[21] F. Yakuphanoglu, Phys. B 388 (2007) 226.
[22] A. Tataroglu, S. Altındal, J. Alloys Compd. 484 (2009) 405.
[23] V. Janardhanam, H.-K. Lee, K.-H. Shim, H.-B. Hong, S.-H. Lee, K.-S. Ahnd, C.-J. Choi, J. Alloys Compd. 504 (2010) 146.

[24] I. Dökme, Ş. Altindal, M. Mahir Bülbül, Appl. Surf. Sci. 252 (2006) 7749.
[25] M.A. Lampert, Rep. Prog. Phys. 27 (1964) 329.
[26] F. Yakuphanoglu, N. Tugluoglu, S. Karadeniz, Phys. B 392 (2007) 188.
[27] A.A.M. Farag, A. Ashery, E.M.A. Ahmed, M.A. Salem, J. Alloys Compd. 495 (2010) 116.
[28] H.M. Zeyada, M.S. Aziz, A.S. Behairy, Phys. B 404 (2009) 3957.
[29] A.A.M. Farag, A. Ashery, E.M.A. Ahmed, M.A. Salem, J. Alloys Compd. 495 (2010) 116.
[30] H. Norde, J. Appl. Phys. 50 (1979) 5052.
[31] Ö. Güllü, A. Türüt, J. Alloys Compd. 509 (2011) 571.
[32] R. Ao, L. Kilmmert, D. Haarer, Adv. Mater. 7 (1995) 495.